European Journal of Pharmaceutical Sciences 222 (2026) 107550

Contents lists available at ScienceDirect

European Journal of Pharmaceutical Sciences

journal homepage: www.elsevier.com/locate/ejps

Cocrystal mitigates the effects of elevated gastric pH on oral absorption of weakly basic drugs: a case study with ketoconazole-succinic acid cocrystal on beagle dogs

Yitian Marguerite Tucci [a,1], Tatiane Cogo Machado [b,1], Duxin Sun [a], Naír Rodríguez-Hornedo [a,*]

[a] Department of Pharmaceutical Sciences, College of Pharmacy, University of Michigan, USA
[b] School of Mathematical and Physical Sciences, Faculty of Science, University of Technology Sydney, Australia

ARTICLE INFO

Keywords:
Supersaturation
Ketoconazole
Cocrystal
pH-dependent
Bioavailability
pH-shift

ABSTRACT

It is well documented that weakly basic drugs, such as ketoconazole (KTZ), will exhibit reduced oral absorption and lower bioavailability in elevated gastric pH conditions. Because this occurs frequently in patients taking medicines to reduce stomach acid, it is crucial to identify formulation strategies that ensure adequate drug exposure. The purpose of this work was to evaluate the *in vitro* and *in vivo* effects of KTZ cocrystals with acidic coformers in mitigating the negative effects of elevated gastric pH on KTZ dissolution and absorption after oral administration. Dissolution-supersaturation-precipitation *in vitro* studies were performed with drug and three KTZ cocrystals with fumaric (FUM), adipic (ADP), and succinic (SUC) acids, under a two-stage pH-shift micro dissolution method, to mimic the transfer from gastric to intestinal compartment. All cocrystals exhibited less sensitivity to elevated gastric pH than the drug. *In vitro*, cocrystals reduced the area under the curve (AUC) 2.6-fold compared to drug where AUC decreased 6.7-fold. Based on the superior performance observed during *in vitro* studies, the KTZ-SUC cocrystal was selected for bioavailability evaluation in beagle dogs treated with pentagastrin and famotidine to simulate normal and elevated gastric conditions. The cocrystal mitigated the negative effects of elevated dog gastric pH on KTZ absorption. It reduced the pH sensitivity of AUC (1.3 times) and C_{max} (1.4 times). The drug exhibited high pH sensitivity with reduced AUC (12.3 times) and C_{max} (7.5 times). These findings demonstrate that cocrystals of weakly basic BCS-class II drugs with acidic coformers promise to improve therapeutic outcomes that are otherwise limited by disease states or co-administration of drugs and food that increase gastric pH.

1. Introduction

The oral absorption of BCS-class II weakly basic drugs is often challenging due to their pronounced pH-dependent solubility (Mitra et al., 2011; Tsume et al., 2017). These therapeutic agents typically exhibit high solubility in the acidic environment of the stomach but undergo a decline in solubility upon transition to the higher pH conditions of the small intestine. This shift often results in supersaturation followed by precipitation, thereby limiting the amount of drug available for absorption across the intestinal membrane (Kostewicz et al., 2004). A well-known example is ketoconazole (KTZ), a weakly basic antifungal agent that has long served as a model compound in numerous absorption studies (Amidon and Tsume, 2017; Higashino et al., 2023; Patel et al., 2019; Ruff et al., 2017; Takano et al., 2006).

Although the clinical KTZ dose (200 mg) is fully dissolved in the stomach (pH ~1–2), it becomes supersaturated and prone to precipitation in the intestinal environment (pH 6–7.5), where KTZ solubility is reduced by orders of magnitude (Chen and Rodríguez-Hornedo, 2018). A young and healthy individual typically has a fasting gastric pH of around 2. In contrast, patients with achlorhydria condition caused by certain diseases (e.g., AIDS, gastric cancer) or the use of gastric acid–suppressing agents may exhibit elevated gastric pH > 5 (Dressman et al., 1990; Mudie et al., 2010; Russell et al., 1993). In humans, KTZ absorption was shown to be markedly reduced with increasing gastric

* Corresponding author.
E-mail address: nrh@med.umich.edu (N. Rodríguez-Hornedo).
[1] Both authors contributed equally to this work.

https://doi.org/10.1016/j.ejps.2026.107550
Received 11 March 2026; Received in revised form 1 May 2026; Accepted 7 May 2026
Available online 8 May 2026

pH. Piscitelli et al. (1991) reported a 95% absorption decrease at gastric pH > 6.0 (Piscitelli et al., 1991). Similarly, Chin et al. (1995) reported a reduction in the area under the curve (AUC) by more than 81% when KTZ was administered in combination with a gastric acid secretion inhibitor (e.g. omeprazole) (Chin et al., 1995). These findings highlight the importance of addressing the pH-dependent absorption of KTZ to ensure adequate drug exposure under conditions of elevated gastric pH.

Strategies to mitigate the pH-effect on the dissolution and absorption of weakly basic drugs have been investigated such as polymeric formulations, lipid-based formulations, and cocrystal formation with acidic coformers (Kuminek et al., 2016; Park et al., 2007; Streubel et al., 2000). A very recent publication by Santos Goes et al. 2026 presented a physiologically based pharmacokinetic (PBPK) approach validated with clinical data of KTZ only (not the cocrystal). The model predicted increased bioavailability of KTZ-SUC cocrystal under elevated gastric pH conditions. Lack of *in vivo* cocrystal data limited validation. We were not aware of this publication until the revision stage of the current manuscript (Santos Goes et al., 2026).

Our earlier studies (Chen and Rodríguez-Hornedo, 2018) demonstrated that cocrystals of KTZ with acidic coformers (succinic (SUC), fumaric (FUM), and adipic (ADP)) improved solubility and dissolution properties by reducing the negative effects of solution pH on KTZ dissolution performance. While these results provided valuable insights for mitigating the effects of elevated pH, they reflect the dissolution–supersaturation–precipitation (DSP) behavior under a one-stage dissolution method (in a single medium).

To better understand how the dissolution advantages of cocrystals may translate to *in vivo* absorption, pH-shift dissolution studies were employed in the present study to simulate the dynamic gastrointestinal environment encountered during oral administration, from the acidic conditions of the stomach to the more elevated neutral pH of the intestine. The pH-shift approach can be used to mimic the dynamic pH changes encountered *in vivo*, making it relevant to evaluating the precipitation behavior and supersaturation maintenance of weakly basic drugs during gastrointestinal transit (Plum et al., 2020). Here, a previously validated micro dissolution pH-shift method (Mathias et al., 2013) was used to investigate the dissolution performance of three 1:1 stoichiometric KTZ cocrystals with acidic coformers, KTZ-ADP, KTZ-FUM, and KTZ-SUC. (Chemical structures and pK_a values of cocrystals components are presented in Table S1). Building on these findings, we demonstrate how the *in vitro* dissolution advantage translates to *in vivo* performance.

The KTZ–SUC cocrystal was selected for pharmacokinetic evaluation in beagle dogs based on its superior KTZ concentration levels during *in vitro* cocrystal dissolution and drug precipitation studies. The dog gastric pH was modulated using pentagastrin, a peptide that stimulates acid secretion and famotidine, a histamine H_2-receptor antagonist that increases gastric pH (Fancher et al., 2011). These pre-treatments allowed for the assessment of KTZ absorption under low pH (acidic) and elevated pH (neutral) conditions, simulating clinically relevant scenarios of patients with normal gastric acidity and patients with achlorhydria due to disease states or oral antacid therapies. The overall aim of this study was to demonstrate the effectiveness of cocrystals on reducing drug absorption variability *in vivo* under unfavorable conditions.

2. Material and methods

2.1. Materials

Racemic KTZ (lot # BS1203355108, 98% purity) was purchased from Bosche Scientific (New Brunswick, NJ) and used as received. ADP (lot # 06807BE, 99% purity), SUC (lot # 037K0021, 99% purity), FUM (lot # 09426EE, 99% purity), acetic acid (lot # 074K3658, 99%), sodium acetate anhydrous (lot # 100K0272), potassium phosphate monobasic (ACS reagent), and sodium chloride (NaCl) (lot # 094K0183, ACS reagent) were purchased from Sigma-Aldrich (St. Louis, MO) and used as received. Fasted state simulated intestinal fluid (FaSSIF) and Fasted state simulated gastric fluid (FaSSGF) powders were purchased from Biorelevant.com (London, United Kingdom) and used as received. HPLC grade methanol, HPLC grade 2-propanol, sodium phosphate monobasic (lot # 017316), and hydrochloric acid (lot # 2AJK15038, ACS grade) were purchased from Fisher Scientific (Fair Lawn, NJ). Acetone (ACS reagent 99.5%) and phosphoric acid (lot # B0506524, 85+%) were purchased from Acros Organics (Morris Plains, NJ) and used as received. Trifluoroacetic acid (spectrophometric grade, 99%) was purchased from Aldrich Company (Milwaukee, WI). Sodium hydroxide (pellets) was purchased from J.T. Baker (Philipsburg, NJ). Deionized water (DI) used in this study was prepared by filtration through a Milli-Q Reference Water System from Millipore Co. (Bedford, MA). Famotidine tablets (Pepsid AC, 10 mg) were purchased over the counter (OTC). Pentagastrin (cat. no. B1636) was obtained from Sigma-Aldrich (St. Louis, MO, USA).

2.2. Methods

2.2.1. Cocrystal synthesis

Cocrystals were prepared by the reaction crystallization method at room temperature (Rodríguez-Hornedo et al., 2006). Acetone was used for KTZ-FUM and KTZ-SUC preparation, and 2-propanol for KTZ-ADP. Full conversion of drug to cocrystal was observed by 24 hours. The solid phases were characterized by X-ray powder diffraction (XRPD), and Differential Scanning Calorimetry (DSC) and compared with those reported by Martin et al. 2013 who discovered the cocrystals. (Table S2 and Fig. S1) (Martin et al., 2013).

2.2.2. Dissolution media preparation

All aqueous media were prepared at room temperature with DI water filtered by Milli-Q Reference Water System. SGF of two different pH values was prepared. HCl (0.01M) solution was prepared for SGF at pH 2.08 ± 0.04. Phosphate buffer (29 mM) was prepared with potassium phosphate monobasic and sodium hydroxide for SGF at pH 6.03 ± 0.03 to represent elevated gastric pH condition. Concentrated FaSSIF and blank FaSSIF (without lecithin and sodium taurocholate) were prepared by using 1.5 times the concentrations of each media component based on the method described by Dressman and coworkers (Galia et al., 1998).

2.2.3. Cocrystal solubility

The equilibrium solubility of each cocrystal was determined at the eutectic point, where both drug and cocrystal solid phases are in equilibrium with the solution (Good and Rodríguez-Hornedo, 2010, 2009). The eutectic points were approached by cocrystal dissolution, where 150 – 200 mg of cocrystal and 50 – 80 mg of KTZ were suspended in 3 mL of blank FaSSIF and FaSSIF. Blank refers to media without surfactants. The solutions were kept in a water bath at 25.0 ± 0.1°C and magnetically stirred for up to 96 hours. Solution samples (0.5 mL) were collected every 24 hours and filtered via cen trifuge through a 0.45 μm pore cellulose acetate membrane, and the pH values were measured. The solid phases were analyzed by XRPD and DSC to confirm that both drug and cocrystal solid phases were present, indicating that the solutions were at the eutectic point. The filtered solutions were then analyzed by HPLC after proper dilutions with the mobile phase.

KTZ and coformer (CF) total (ionized + non-ionized) concentrations at the eutectic points were used to calculate the cocrystal stochiometric solubility values ($S_{cc,T}$) according to

$$S_{cc,T} = \sqrt{[\mathrm{KTZ}]_{eu,T}[\mathrm{CF}]_{eu,T}} \quad (1)$$

where the terms in brackets refer to molar concentrations and the subscript “eu” indicates eutectic point.

The equations used to determine the cocrystal solubility dependence on drug and coformer solubilization and ionization are presented in the

supplementary material.

2.2.4. pH-shift dissolution

The dissolution test was based on the micro dissolution pH-shift test developed by Mathias et al. (Mathias et al., 2013). The pH-shift dissolution was conducted in two stages, to mimic the transfer from gastric to intestinal compartment. In our work, two pH shift conditions were investigated, $SGF_{pH\ 2} \rightarrow FaSSIF_{pH6.5}$ and $SGF_{pH6} \rightarrow FaSSIF_{pH6.5}$, that correspond to normal and elevated gastric pH.

Drug and cocrystals were first added to 7 mL of SGF at pH 2 (normal) or pH 6 (elevated). At 20 min, 14 mL of the concentrated (1.5 x) FaSSIF was added to cause a pH-shift to pH 6.5, and dissolution monitored for 180 minutes. The mass of solid used for drug and cocrystal dissolution translates to concentrations between 1.5 mM and 1.6 mM (corresponding to the 200 mg KTZ dose/250 mL) in the initial SGF media (pH 2) and becomes approximately 0.5mM following dilution by the addition of the second media (pH 6.5). Dissolution was conducted in a 25 mL beaker with magnetic stirring (200 rpm) set in a water bath at 24.8 ± 0.2°C. This temperature is consistent with that used in all *in vitro* cocrystal studies in our laboratory of about 25°C allowing for correlation between thermodynamic and kinetic findings. The drug and cocrystal solids used were sieved to obtain particles between 106 – 125 μm. Aliquots of approximately 0.4 mL were collected with a syringe at selected time points both prior to and following the pH-shift. Aliquot volume was not replaced. Loss in volume of the initial dissolution media was accounted for in the calculation of theoretical maximum concentrations based on the fully dissolved dose. The solution samples were filtered using syringe filter with PVDF membrane of 0.45 μm pore size. The solution concentrations of drug and coformers were analyzed by HPLC after proper dilution with mobile phase. pH during dissolution was monitored. The initial pH values (before pH shift) ranged from 2.21 to 2.23 for SGF_{pH2}, 5.89 to 6.04 for SGF_{pH6}, and 6.15 to 6.36 for $FaSSIF_{pH6.5}$. The final pH values (after pH shift) are shown in Table 1.

2.2.5. pH-effect

The *in vitro* pH-effect was calculated using the following equation:

$$\text{pH effect}_{(in\ vitro)} = \frac{AUC_{(SGF_{pH6} \rightarrow FaSSIF_{pH6.5})}}{AUC_{(SGF_{pH2} \rightarrow FaSSIF_{pH6.5})}} \quad (2)$$

Where $AUC_{(SGFpH6 \rightarrow FaSSIFpH6.5)}$ is the area under the curve (AUC) of the KTZ concentration versus time from the dissolution profiles of elevated gastric pH to intestinal transfer, and $AUC_{(SGFpH2 \rightarrow FaSSIFpH6.5)}$ of normal gastric pH to intestinal transfer. The *in vitro* AUC was determined by integration of the KTZ concentration versus time profiles from 20 to 180min, corresponding to the AUC after the pH shift.

The *in vivo* pH-effect was calculated using the following equation:

$$\text{pH effect}_{(in\ vivo)} = \frac{AUC_{(famotidine)}}{AUC_{(pentagastrin)}} \quad (3)$$

Where $AUC_{(famotidine)}$ refers to the area under the plasma concentration–time curve for KTZ in dogs treated with famotidine to simulate elevated gastric pH (5–7.5) and $AUC_{(pentagrastrin)}$ refers to the area under the plasma concentration–time curve for KTZ in dogs treated with pentagastrin, which simulates a low gastric pH (2–3).

Table 1
Final dissolution pH, KTZ C_{max} and σ_{max}, following pH-shift.

Sample	Solution media	Final pH	C_{max} (mM)	σ_{max} [a]
KTZ	$SGF_{pH\ 2} \rightarrow FaSSIF_{pH6.5}$	6.36 ± 0.01	0.516 ± 0.005	14.3 ± 0.1
	$SGF_{pH6} \rightarrow FaSSIF_{pH6.5}$	6.33 ± 0.01	0.046 ± 0.002	1.25 ± 0.06
KTZ-ADP	$SGF_{pH\ 2} \rightarrow FaSSIF_{pH6.5}$	6.29 ± 0.01	0.515 ± 0.008	13.6 ± 0.2
	$SGF_{pH6} \rightarrow FaSSIF_{pH6.5}$	6.31 ± 0.01	0.230 ± 0.008	6.2 ± 0.2
KTZ-FUM	$SGF_{pH\ 2} \rightarrow FaSSIF_{pH6.5}$	6.30 ± 0.01	0.518 ± 0.008	13.8 ± 0.2
	$SGF_{pH6} \rightarrow FaSSIF_{pH6.5}$	6.28 ± 0.01	0.22 ± 0.01	5.8 ± 0.3
KTZ-SUC	$SGF_{pH\ 2} \rightarrow FaSSIF_{pH6.5}$	6.29 ± 0.01	0.512 ± 0.004	13.6 ± 0.1
	$SGF_{pH6} \rightarrow FaSSIF_{pH6.5}$	6.29 ± 0.01	0.29 ± 0.02	7.7 ± 0.7

[a] $\sigma_{max} = (C_{max}/S)_{drug}$. S_{drug} values are predicted from KTZ solubility vs pH equations as shown in Fig. 1 and Supplementary material.

2.2.6. In vivo oral administration study in beagle dogs

The animal study was approved by the Institutional Animal Care & Use Committee (IACUC) at the University of Michigan. Beagle dogs (10-15 kg) were allocated into two groups under the condition of pentagastrin and famotidine pretreatment groups. The same group of three dogs was used in pentagastrin and famotidine groups consecutively. A washout period of one week was maintained between consecutive administrations. The dogs were fasted overnight, and no food intake occurred 4 h after dosing.

Capsules containing cocrystal and pure drug were orally administered at a dose of 50 mg equivalent drug to the dogs in each group (famotidine and pentagastrin) by gavage with 50 mL of water (corresponding to 1.88 mM KTZ). Dogs were not allowed water intake 1 h before dosing and 1 h after dosing.

The pentagastrin group was intramuscularly treated with pentagastrin (6 mg/kg) 0.5 h before dosing to avoid variability of gastric pH among individual dogs and keep pH values between 2 and 3. The famotidine group was treated with (40 mg/dog). Four tablets of 10 mg famotidine were administered orally 3 hours before dosing to maintain gastric pH values at 5-7.5. Blood samples (~200 μL) were collected at 0, 0.5, 1, 2, 4, 6 and 24 hours and then centrifuged, and analysed by Liquid Chromatography with Mass Spectrometry (LC-MS/MS).

Pharmacokinetic parameters determined for KTZ included maximum plasma concentration (C_{max}), time to reach the maximum plasma concentration (T_{max}) and area under the plasma concentration-time curve from time zero to the time of the last quantifiable concentrations (AUC_{0-t}), measured by linear trapezoidal method. The pharmacokinetic parameters were determined by non-compartmental methods using Phoenix WinNonlin.

2.2.7. Analysis of plasma concentration

The concentrations of KTZ in dog plasma were quantified by LC-MS/MS using a XBridge C18 (Waters) 5 cm x 2.1 mm I.D. column, packed with 5.0 μm connected to an LC/MS/MS. Elution was accomplished using a linear gradient delivered at 0.4 mL/min that consisted of ramping 0.1% formic acid in DI water (solution A) and 0.1% formic acid in acetonitrile (solution B) at a ratio of 95% A at 0-0.5 min, 5% A at 1.50-3.50 min and 95% A at 3.60 to 5.60 min. The MS/MS instrument was operated in electrospray ionisation mode. Detection was performed in the positive-ion mode using selected reaction monitoring of transition from m/z 531.1 to 489.1.

3. Results and discussion

3.1. In vitro pH-shift dissolution studies

The *in vitro* pH-shift dissolution test was conducted for drug and cocrystals to simulate biorelevant conditions encountered in transfer from the gastric to intestinal compartments. Two pH-shift conditions were considered: $SGF_{pH2} \rightarrow FaSSIF_{pH6.5}$, to simulate the transfer from normal gastric pH to intestinal stage, and $SGF_{pH6} \rightarrow FaSSIF_{pH6.5}$, to simulate elevated gastric pH to intestinal stage transfer.

3.1.1. $SGF_{pH2} \rightarrow FaSSIF_{pH6.5}$

Fig. 1 shows the drug and cocrystals solubility *vs* pH in buffer and in FaSSIF as well as the KTZ concentrations that can be achieved during drug and cocrystal dissolutions during pH-shift studies from $SGF_{pH2} \rightarrow FaSSIF_{pH6.5}$. KTZ solubility is highly pH-dependent due to its basic nature ($pK_{a1} = 3.17$ and $pK_{a2} = 6.63$)(Avdeef, 2012). Drug and cocrystal solubilities are higher in FaSSIF than in blank FaSSIF of the same pH. The dose used (0.8 mg KTZ equivalent) per mL in the initial media, leads to KTZ concentration (fully dissolved dose) of 1.5 mM before pH-shift and 0.5 mM after pH-shift, due to the volume increase. At the initial pH (~ 2.2), both drug and cocrystal dose can fully dissolve as the maximum concentration is below their solubility, therefore no supersaturation with respect to KTZ is generated until the pH shift. After the pH-shift to $FaSSIF_{pH\ 6.5}$, KTZ solubility decreased dramatically, and the dose if fully dissolved would generate supersaturation ($\sigma_{theoretical}$) values between 13 and 14. $\sigma > 1$ indicates that the solution is supersaturated with KTZ and precipitation of drug is thermodynamically favourable. The range of σ values is due to the slight pH variations in dissolution studies. $\sigma_{theoretical}$ values for each condition are shown in supplementary material (Table S5).

The $SGF_{pH2} \rightarrow FaSSIF_{pH6.5}$ pH shift dissolution results are shown in Fig. 2 as drug concentration and supersaturation ($\sigma = (C/S)_{drug}$) *vs* time. C_{drug} refers to drug concentration measured during dissolution and S_{drug} refers to drug equilibrium solubility at the corresponding final dissolution pH (Table 1). KTZ concentrations of 0.5 mM indicated that full cocrystal and drug dissolution had occurred in the first 20 minutes of the experiment before the pH was shifted. Plots of % solid drug and cocrystal dissolved before and after pH shifts are included in the supplementary material (Fig. S2). Bulk pH values were similar for drug and cocrystal dissolutions, and they increased from around 2.2 before to about 6.3 after the pH-shift (Table 1). All solutions remained clear, and no cloudiness or precipitation was observed following the pH-shift.

The maximum supersaturation levels (σ_{max}=13-14), obtained from $\sigma_{max} = (C_{max}/S)_{drug}$, were sustained for 75 min for KTZ-SUC, for 60 min for KTZ-ADP and KTZ-FUM, and for 50 min for KTZ drug. By the end of the dissolution (180 min), KTZ concentrations obtained from the cocrystals remained supersaturated at levels between 3 and 4. Although the cocrystal and the drug exhibited similar C_{max} values (Table 1), the total dissolution $AUC_{(20–180min)}$ values (Table 2) were higher for the cocrystal as a result of prolonged supersaturation. The kinetics of precipitation can vary greatly due to many factors, including not only the degree of supersaturation but also pH, solution composition, stirring, and temperature (Leyssens and Horst, 2018).

3.1.2. $SGF_{pH6} \rightarrow FaSSIF_{pH6.5}$

Fig. 3 presents the drug and cocrystals solubility vs pH curves in buffer and FaSSIF as well as the KTZ concentrations that can be achieved during drug and cocrystals dissolution during pH-shift studies from $SGF_{pH6} \rightarrow FaSSIF_{pH6.5}$. This plot shows that at the initial pH of around 6 the cocrystals can fully dissolve but the KTZ crystal does not. Cocrystals can generate supersaturation with respect to KTZ of $\sigma_{theoretical}$ values between 52 and 66, when fully dissolved and without drug precipitation. Such supersaturation levels can lead to a solution-mediated precipitation to KTZ prior to the pH-shift. This is in contrast to the behavior when the initial pH is 2 (Fig. 1) where the solutions are undersaturated with respect to KTZ.

After the pH-shift to FaSSIF pH 6.5, $\sigma_{theoretical}$ decreases to values between 12 to 14. In this case, the measured pH increases from initial to final media was relatively small (< 0.5 pH units), and drug solubility is higher in final media ($FaSSIF_{pH6.5}$) compared to initial media (SGF_{pH6}) due to the solubilizing effect of FaSSIF. The solid could either be from undissolved drug/cocrystal or from cocrystal conversion to drug. The amount of solids obtained in our studies was insufficient for analytical characterization.

KTZ exhibits a 4.7-fold increase in solubility in FaSSIF compared to blank FaSSIF at a pH_{eq} of 6.5 (Bevernage et al., 2012; Chen, 2017). Cocrystal solubility in surfactant media was much lower than that of drug, ranging between 1.1 and 1.4. due to the lower pH_{eq} values (4.1-4.5) during solubility measurements. Acidic coformers decreased the solubility media pH from the initial value of 6.5. Although KTZ has demonstrated poor solubility, dissolution, and oral absorption at elevated gastric pH (Dressman and Reppas, 2000; Van der Meer et al.,

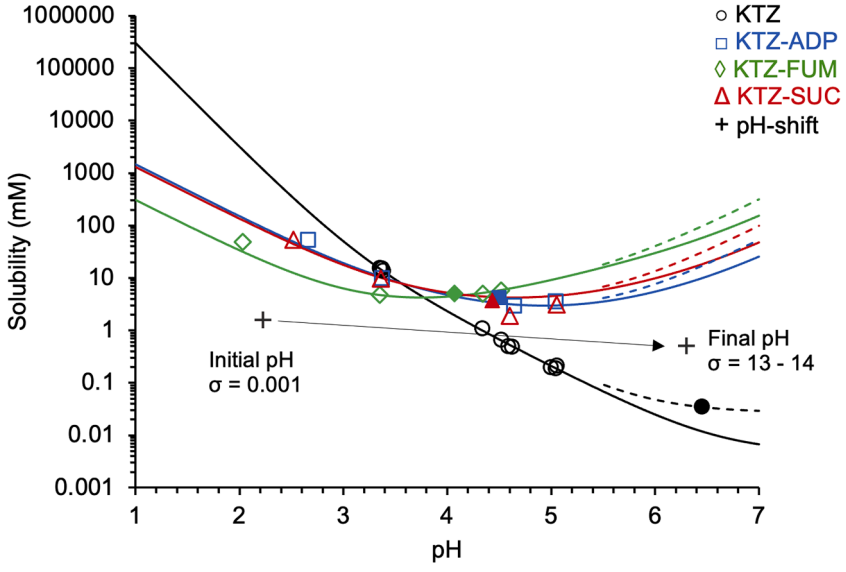

Fig. 1. Drug and cocrystals solubility *vs* pH in buffer and in FaSSIF. This diagram shows the KTZ concentrations that can be achieved during drug and cocrystals dissolution during pH-shift $SGF_{pH2} \rightarrow FaSSIF_{pH6.5}$. Solid curves represent KTZ and cocrystals solubility-pH profiles generated using equations and parameter values previously published (Chen and Rodríguez-Hornedo, 2018). Dashed lines represent the influence of surfactants in FaSSIF on drug and cocrystal solubility and were calculated according to equations and parameter values presented in Supplementary material. Open symbols indicate experimental solubility in aqueous buffer, and closed symbols represent solubility in FaSSIF. The standard errors of experimental solubility values are less than 4% and are within the data symbol. Concentrations of drug before and after pH-shift are indicated by "+", and pH-shift is indicated by "→". σ in this plot represents the theoretical supersaturation with respect to KTZ ($\sigma_{theoretical}$) if dose is fully dissolved. Initial $\sigma = 0.001$ and final $\sigma = 13$-14, and it is equal to $(C/S)_{drug}$. The range of σ values is due to the slight pH variations from the dissolution studies.

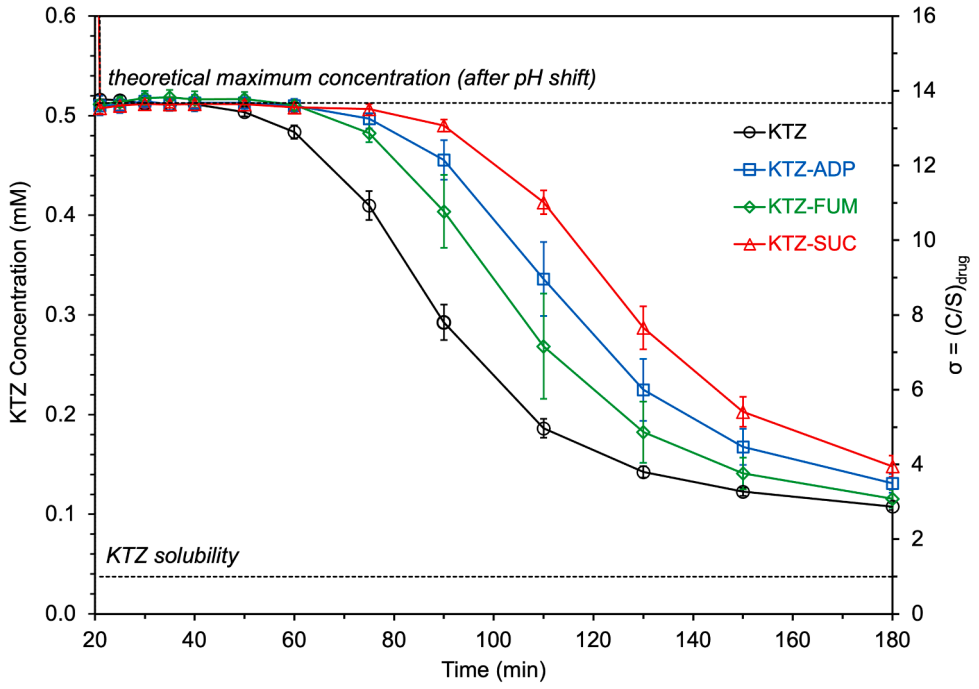

Fig. 2. KTZ concentration and supersaturation *vs* time profiles after pH-shift from SGF_{pH2} → $FaSSIF_{pH6.5}$ (20-180min). The top dashed line denotes the KTZ concentration and supersaturation if the drug and cocrystals fully dissolved. The bottom dashed line indicates drug solubility where σ =1.

Table 2
KTZ AUC after pH shift (20-180min) for drug and cocrystal dissolution, AUC ratio of cocrystal to drug, and the pH-effect obtained from the AUC ratio between elevated gastric pH to normal pH conditions.

Sample	*In vitro* condition	$AUC_{(20\text{-}180min)}$ (mM x min)	AUC ratio (cc/drug)	pH-effect *in vitro*[a]
KTZ	$SGF_{pH\ 2}$ → $FaSSIF_{pH6.5}$	46 ± 1	-	0.15 ± 0.01
	SGF_{pH6} → $FaSSIF_{pH6.5}$	7.0 ± 0.4	-	
KTZ-ADP	$SGF_{pH\ 2}$ → $FaSSIF_{pH6.5}$	57 ± 2	1.23 ± 0.06	0.40 ± 0.02
	SGF_{pH6} → $FaSSIF_{pH6.5}$	23 ± 1	3.2 ± 0.2	
KTZ-FUM	$SGF_{pH\ 2}$ → $FaSSIF_{pH6.5}$	53 ± 3	1.14 ± 0.07	0.39 ± 0.03
	SGF_{pH6} → $FaSSIF_{pH6.5}$	20 ± 1	2.9 ± 0.2	
KTZ-SUC	$SGF_{pH\ 2}$ → $FaSSIF_{pH6.5}$	61.2 ± 0.8	1.33 ± 0.04	0.40 ± 0.04
	SGF_{pH6} → $FaSSIF_{pH6.5}$	24 ± 2	3.5 ± 0.4	

[a] pH effect obtained from the AUC ratio between elevated gastric condition ($_{SGFpH6→FaSSIFpH6.5}$) to normal gastric condition (SGF_{pH2}→$FaSSIF_{pH6.5}$).

1980; Zhou et al., 2005), all three cocrystals studied have higher solubilities and dissolution advantages over the drug, which would reflect in improved *in vivo* absorption. We have shown that cocrystals have a dissolution advantage over KTZ ranging from 30 to 200 times at bulk pH of 5 to 6 based on flux determinations from intrinsic dissolution studies in buffered media without surfactant (Cao et al., 2019). It is also interesting to note that cocrystals modulated the interfacial pH. At bulk pH values of 4 to 7, the KTZ-SUC cocrystal interfacial pH is 4.5. This lower pH value is favorable for both higher solubility and flux of the cocrystal.

Fig. 4 shows that KTZ concentrations from cocrystal dissolution increased immediately after the pH shift, indicating the presence of undissolved cocrystal after the shift. This is further supported by the observation that concentrations did not reach the theoretical maximum concentration (dashed line). In contrast, the pure drug exhibited lower dissolution rates, resulting in lower concentrations compared to the cocrystals.

The percentage dose dissolved for drug and cocrystals is presented in Fig. S2 and Table S6. Fig. 4 also shows dissolution findings expressed as supersaturation. Maximum supersaturation (σ_{max}) was achieved at 35 minutes for all cocrystals, after which it decreased to levels around 2.5 by the end of the experiment at 180-minutes. The highest supersaturation (σ_{max} = 7.7) was observed for KTZ-SUC, followed by KTZ-ADP (σ_{max} = 6.2) and KTZ-FUM (σ_{max} = 5.8). These results are also presented in Fig. 5A. Elevated gastric pH condition is where the KTZ cocrystals truly demonstrated advantages over the drug. While the weakly basic drug struggled to dissolve under the high pH conditions, the cocrystals were able to generate much higher drug concentrations.

3.1.3. *Dissolution key parameters: C_{max}, σ_{max} and AUC*

A summary of the dissolution findings under both pH-shift conditions, in terms of C_{max}, σ_{max} and AUC is presented in Fig. 5 and Tables 1 and 2. C_{max} from drug and cocrystals dissolutions in SGF_{pH2} → $FaSSIF_{pH6.5}$ are not statistically different, which means cocrystal does not offer advantage at normal gastric pH conditions, in which the basic drug is highly soluble. As shown in Fig. 1, KTZ solubility at this pH (~2) is higher than that of the cocrystals and sufficient to dissolve the full therapeutic dose; therefore, no improvement is needed, as dissolution is not a limiting factor.

Table 2 presents the *in vitro* dissolution AUC ratios between cocrystal and drug demonstrating the cocrystal dissolution advantage over drug, and this is shown for both normal and elevated gastric pH conditions in Fig. 5B. Overall, cocrystals showed reduced sensitivity to elevated gastric pH relative to the drug, as demonstrated by higher dissolved KTZ concentrations and AUC ratios ranging from 2.9- to 3.5-fold, in SGF_{pH6}→

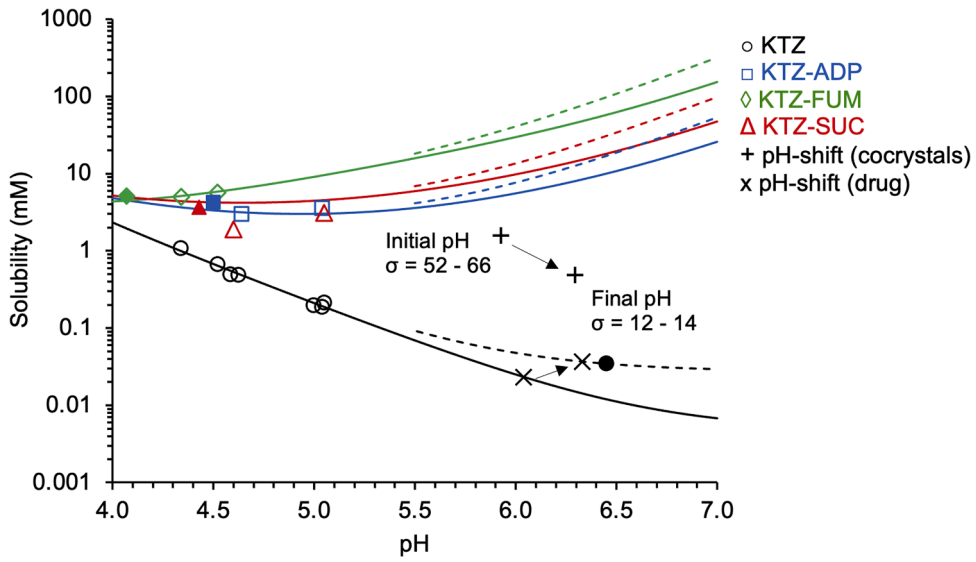

Fig. 3. Drug and cocrystals solubility vs pH curves in buffer and FaSSIF. This diagram shows the KTZ concentrations that can be achieved during drug and cocrystals pH-shift $SGF_{pH6} \rightarrow FaSSIF_{pH6.5}$ dissolutions. Solid curves represent KTZ drug and cocrystal solubility-pH profiles from pH 4 to 7. The influence of surfactants in FaSSIF on drug and cocrystal solubility is represented as dashed lines. Open symbols indicate experimental solubility in aqueous buffer, and closed symbols represent solubility in FaSSIF. The standard errors of experimental solubility values are less than 4% and are within the data symbol. KTZ concentrations from cocrystal dissolution before and after pH-shift are indicated by "+", and from drug dissolution are indicated by "x". pH-shift is indicated by "→". σ in this plot represents the theoretical supersaturation level ($\sigma_{theoretical}$) of KTZ if drug or cocrystal is fully dissolved. σ = 52-66 before pH-shift and σ = 12-14 after. Solubility-pH profiles were generated using equations and parameter values previously published (Chen and Rodríguez-Hornedo, 2018). The influence of FaSSIF on drug and cocrystal solubility is represented as dashed lines generated from equations and parameter values presented in Supplementary material.

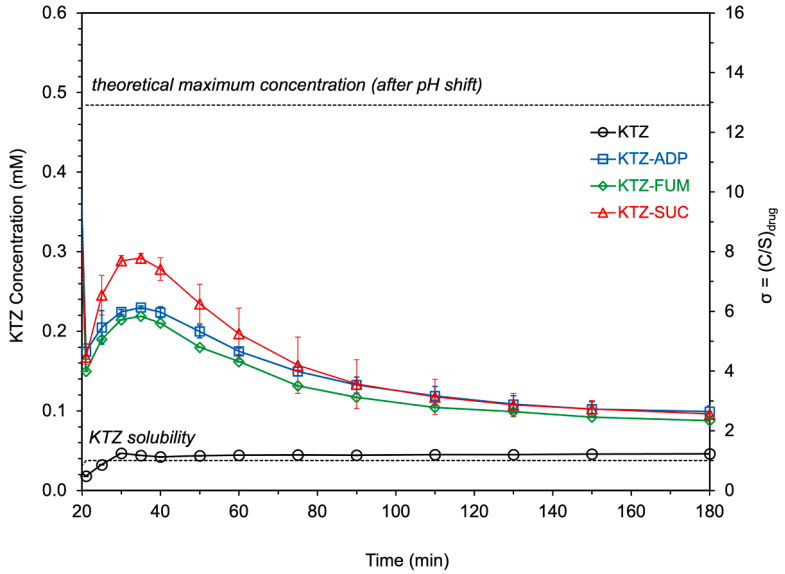

Fig. 4. KTZ concentration and supersaturation vs time profiles after pH-shift from $SGF_{pH6} \rightarrow FaSSIF_{pH6.5}$ (20-180min). The top dashed line denotes the maximum theoretical concentration if the full cocrystal and drug are dissolved. The bottom dashed line indicates drug solubility, where σ =1. Cocrystals cannot dissolve the full dose and reach the theoretical dashed line because drug precipitates at σ between 6-8.

$FaSSIF_{pH6.5}$ condition. Notably, the highest σ_{max} (7.7) for KTZ–SUC corresponded to the largest AUC enhancement (3.5-fold), supporting its selection for subsequent *in vivo* studies.

3.1.3.1. AUC ratio between conditions as an indicator of pH-effect in vitro. The KTZ pH-dependent dissolution was assessed by considering the AUC ratio between elevated and normal gastric pH conditions ($AUC_{SGFpH6 \rightarrow FaSSIF}/AUC_{SGFpH2 \rightarrow FaSSIF}$), according to equation (2). When the ratio =1, there is no pH-effect. This analysis has been previously presented by Mathias et al. (Mathias et al., 2013) for a variety of weakly basic drugs, including KTZ and it is referred to as the pH-effect ratio. The pH-effect ratio for KTZ from our pH-shift dissolution studies was found to be 0.15, and it is compared to the *in vitro* AUC ratio of 0.22 reported by Mathias et al. under similar micro dissolution study (0-180min) (Mathias et al., 2013). The AUC in our work was determined after pH shift (20 to 180 min), and they are still relevant to evaluate the effect of gastric pH on KTZ exposure in the intestinal environment. The pH-effect ratios for cocrystals KTZ-ADP, KTZ-FUM, and KTZ-SUC are 2.7 times higher than the drug. Larger ratio values of the cocrystals indicate that the pH-effect for cocrystals is less pronounced than for the drug. Therefore, cocrystals could provide the advantage of mitigating *in vivo* pH effects. (Fig. 6)

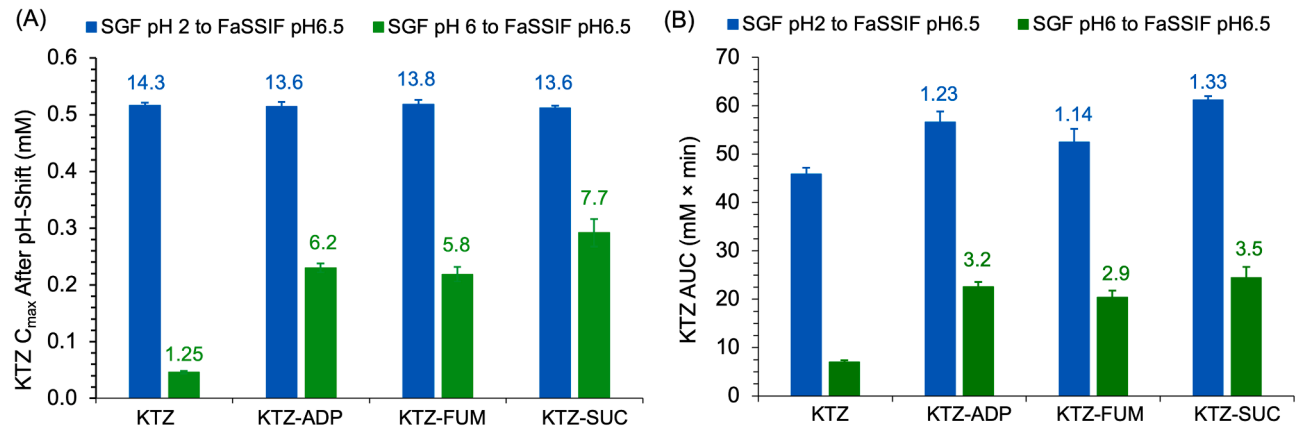

Fig. 5. (A) KTZ C_{max} after pH-shift for drug and cocrystal dissolution. Numbers on top of columns indicate σ_{max} values $(C_{max}/S)_{drug}$. pH values in the legend indicate initial media pH. Error bars indicate standard errors. No statistically significant differences in C_{max} for cocrystals and drug pH-shift dissolutions starting with SGF pH2. ($p>0.05$). (B) KTZ AUC after pH-shift (20 – 180 min) for drug and cocrystal dissolution. Number on top of the column indicates AUC ratio of cocrystal to drug ($AUC_{cc/drug}$). Cocrystals exhibited dissolution advantage related to pure drug under elevated pH conditions with ratio ranging from 2.9 to 3.5.

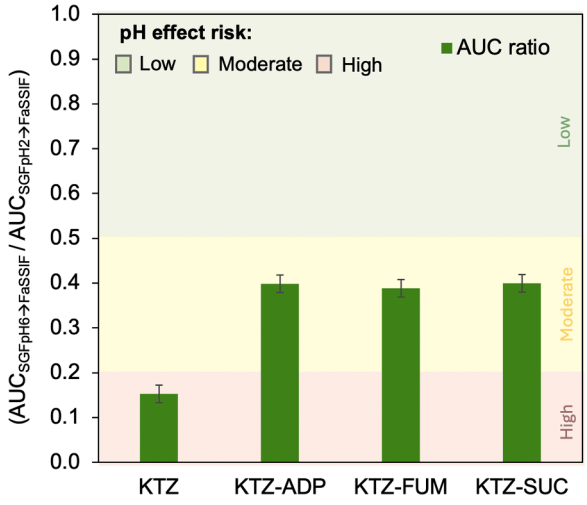

Fig. 6. *In vitro* AUC ratio between elevated and normal gastric pH conditions from pH-shift studies. AUC ratio = $(AUC_{SGFpH6\rightarrow FaSSIF}/AUC_{SGFpH2\rightarrow FaSSIF})$. Cocrystals reduced the pH-dependent dissolution effect of KTZ at elevated gastric pH, lowering the pH-effect from high to moderate *in vitro*. High, Moderate and Low categories are based on the pH-effect risk assessment proposed by Mathias et al. (Mathias et al., 2013).

3.2. *In vivo studies*

Table 3 and Fig. 7 illustrate the drug mean plasma concentration-time profiles following a single oral gavage administration of KTZ and KTZ-SUC to dogs pre-treated with famotidine and pentagastrin. In fasted beagles, the gastric pH corresponding to the administered doses of famotidine and pentagastrin are expected to be approximately (pH 5-7.5) and (pH 2-3), respectively (Koziolek et al., 2019). Fasting gastric pH was reported to be >5 in healthy elderly humans taking 40mg famotidine (Russell et al., 1993).

The pharmacokinetics of KTZ were significantly affected by famotidine administration. As gastric pH increases, KTZ solubility decreases, leading to reduced KTZ available for absorption. This resulted in a decrease in C_{max}, from $(6 \pm 3) \times 10^3$ ng/mL under pentagastrin treatment to $(0.8 \pm 0.2) \times 10^3$ ng/mL with famotidine, representing a 7-fold reduction. These findings align with previous studies, which investigated pH-dependent effects on KTZ absorption in dogs (Zhou et al., 2005). For instance, Van der Meer et al. (1980) reported that a 200 mg oral dose of KTZ in humans led to peak plasma concentrations approximately five times lower when co-administered with cimetidine and sodium bicarbonate (antacid therapy) compared to fasting conditions (Van der Meer et al., 1980). As expected, KTZ exhibits greater solubility at pH 2 than at pH 6.5, favoring dissolution and absorption in acidic conditions. When KTZ-SUC was administered to famotidine-treated dogs, plasma concentrations peaked at $(6 \pm 1) \times 10^3$ ng/mL, which is comparable to C_{max} observed for KTZ under acidic gastric pH, condition where absorption is favorable for KTZ ($p > 0.05$). This means the cocrystal mitigated the negative impact of increased gastric pH, leading to a C_{max} 7 times higher than that of pure KTZ under the same conditions and, 11-fold AUC improvement (Fig. 8).

3.3. *pH-effect risk and in vitro-in vivo correlations*

The pH-effect *in vitro* based on the AUC ratio between conditions was previously shown in Fig. 6 to indicate the risk of elevated gastric pH on drug and cocrystals dissolution-supersaturation-precipitation. KTZ-SUC increased the *in vitro* AUC ratio from 0.15 (KTZ crystal) to 0.40,

Table 3
Pharmacokinetic parameters for KTZ and cocrystals in dogs under pentagastrin and famotidine treatment conditions. (n=3).

	Parameters, mean ± SD or median (range)			
	C_{max} [a] (10^3 ng/mL)	T_{max} [b] (h)	$AUC_{(0\text{-}24h)}$ [c] (10^3 ng h/mL)	t ½ (h) [d]
KTZ (pentagastrin)	6 ± 3	2 (1 – 4)	37 ± 7	2.18
KTZ-SUC (pentagastrin)	8.4 ± 0.9	1 (1 – 2)	48 ± 4	2.28
KTZ (famotidine)	0.8 ± 0.1	2 (2– 2)	3.3 ± 0.4	3.53
KTZ-SUC (famotidine)	6 ± 1	1 (0.5 – 2)	37 ± 6	2.80

[a] C_{max} = Maximum observed concentration.
[b] T_{max} = time of maximum observed plasma concentration. Values are reported as median and range (n=3).
[c] $AUC_{(0\text{-}24h)}$ = Area under the concentration-time curve from time zero to 24h.
[d] Terminal elimination half-life (t ½) was calculated based on data points (≥3) in the terminal phase with correlation coefficient >0.90.

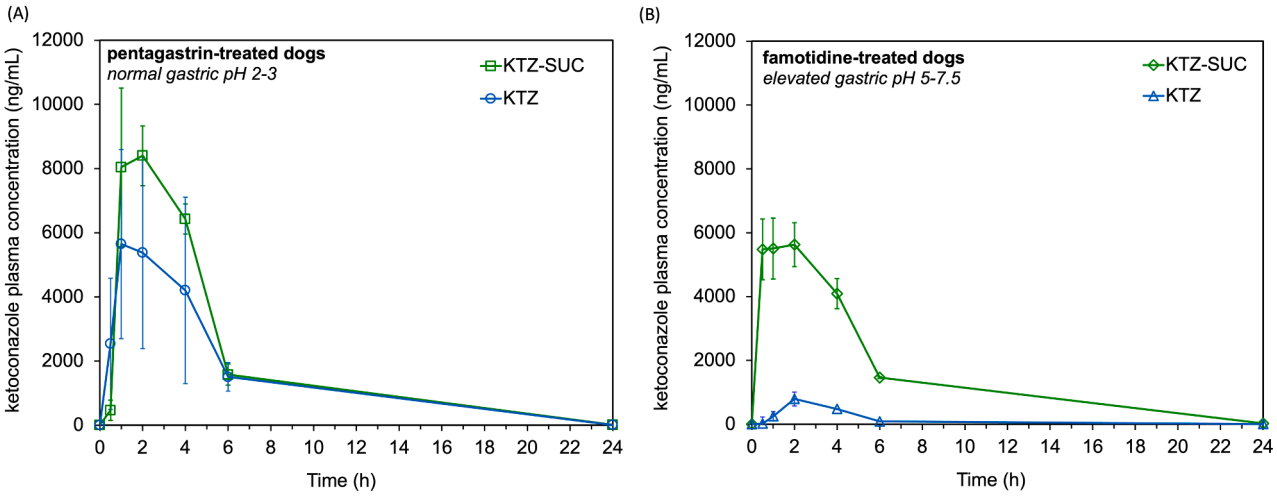

Fig. 7. KTZ plasma concentration versus time after oral administration of KTZ and KTZ-SUC at a dose of 50 mg to fasted dogs treated with pentagastrin (A) and famotidine (B) (n=3, mean ± S.D.).

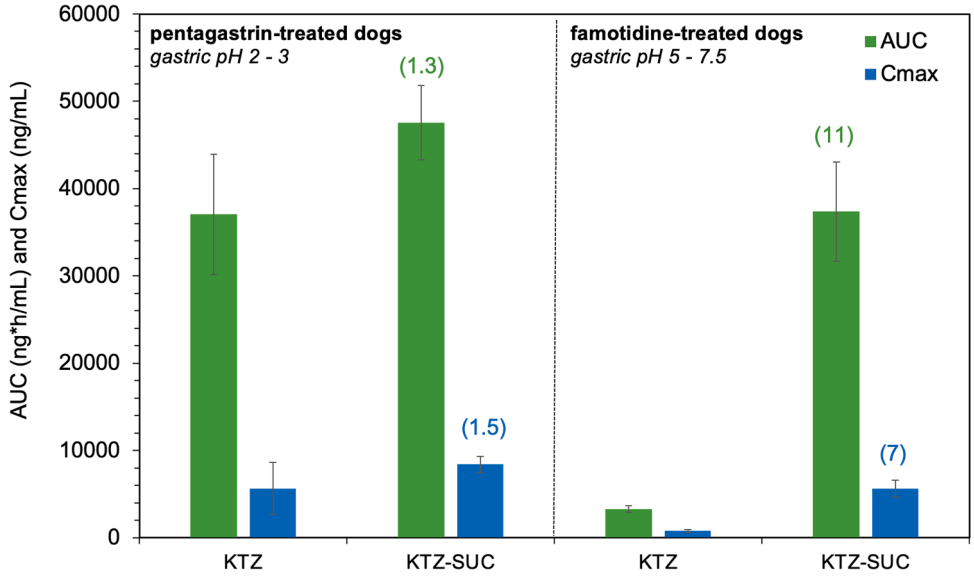

Fig. 8. Pharmacokinetic parameters ($AUC_{0\text{-}24h}$ and C_{max}) for KTZ and KTZ-SUC dosed to dogs treated with pentagastrin and famotidine (n = 3 dogs/group, mean ± S.D.). The numbers above KTZ-SUC bars are the AUC and C_{max} ratio of cocrystal to drug. Higher ratios in famotidine treated condition indicate cocrystal ability to mitigate the impact of pH on drug pharmacokinetics affected by famotidine due to the increase in gastric pH.

indicating cocrystal potential for mitigating the pH-effect *in vivo*. We now compare the *in vitro* pH-effect ratio with the pH-effect ratio obtained from the dog *in vivo* study and classify them according to the pH-effect risk assessment proposed by Mathias et al. (Fig. 9). *In vitro* and *in vivo* pH-effect risk is categorized as follow: *in vitro* AUC ratio >0.5 as low risk (equivalent to *in vivo* C_{max} or AUC ratio > 0.8); *in vitro* AUC ratio of 0.2–0.5 as moderate risk (equivalent to *in vivo* C_{max} and AUC ratio of 0.5-0.8); and *in vitro* AUC ratio <0.2 as high risk (equivalent to *in vivo* C_{max} and AUC ratio <0.5) (Mathias et al., 2013). pH-effect risk categories are illustrated in Fig. 9 to facilitate clearer visualisation of the cocrystal superior performance and the differences between *in vitro* and *in vivo*. AUC and C_{max} ratio values are included in Table 4. A ratio of 1 represents no pH effect. The smaller the ratio, the stronger the influence of elevated gastric pH on drug exposure and absorption.

KTZ-SUC reduced the risk of pH-effect from high to moderate *in vitro* and from high to nearly low *in vivo*. This is supported by the increase in the *in vivo* AUC ratio from 0.09 to 0.79. In contrast, the KTZ-SUC performance *in vitro* resulted in an AUC ratio of 0.40, almost half of the AUC ratio from *in vivo* study. The superior cocrystal performance *in vivo* can be attributed to the absorptive environment present *in vivo*, which is absent under the non-sink conditions of the pH-shift dissolution method used in this work. Drug supersaturation and precipitation are often overestimated in such *in vitro* dissolution setups because they lack an absorption compartment (Bevernage et al., 2012). *In vivo*, the free drug is continuously removed through absorption, which may reduce the risk of drug precipitation leading to higher AUC ratio, as observed with the *in vivo* dog studies. While each method has its own advantages and limitations, the findings presented here support the *in vitro* micro dissolution pH-shift method as a powerful tool for screening cocrystals with a high probability of success *in vivo*.

4. Conclusion

This study demonstrates that cocrystals of BCS-class II weakly basic drugs with acidic coformers can effectively mitigate the negative effects that elevated gastric pH have on oral drug absorption. The *in vitro* pH-

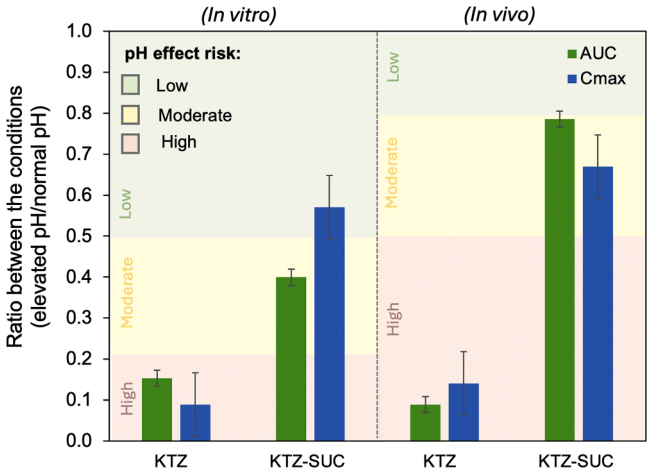

Fig. 9. pH-effect risk categories based on *in vitro* dissolution and *in vivo* key parameters, C_{max} and AUC expressed as a ratio between conditions (elevated pH to normal gastric pH). Cocrystal reduce drug pH-effect sensitivity from high to moderate *in vitro*, and high to moderate-low *in vivo*.

Table 4
pH-effect ratio between initial pH 2 or pH6 and FaSSIF for the *in vitro* and *in vivo* studies of KTZ and KTZ-SUC. Higher values closer to 1 indicate less sensitivity of dissolution and absorption to elevated gastric pH.

	In vitro (pH-shift study)		*In vivo* (dog study)	
Sample	AUC ratio[a]	C_{max} ratio[b]	AUC ratio[c]	C_{max} ratio[d]
KTZ	0.15 ± 0.01	0.09 ± 0.01	0.09 ± 0.02	0.14 ± 0.08
KTZ-SUC	0.40 ± 0.04	0.57 ± 0.08	0.8 ± 0.1	0.67 ± 0.08

[a] *In vitro* AUC ratio from pH-shift dissolutions ($AUC_{SGFpH6\rightarrow FaSSIF}$/$AUC_{SGFpH2\rightarrow FaSSIF}$).
[b] *In vitro* C_{max} ratio from pH-shift dissolutions ($C_{max,\ SGFpH6\rightarrow FaSSIF}$/$C_{max,\ SGFpH2\rightarrow FaSSIF}$).
[c] *In vivo* AUC ratio from dog studies ($AUC_{(famotidine)}$ / $AUC_{(pentagrastrin)}$)
[d] *In vivo* C_{max} ratio from dog studies ($C_{max(famotidine)}$ / $C_{max(pentagrastrin)}$)

shift dissolution studies, designed to mimic the transition from gastric conditions (normal pH 2 and elevated pH 6) to the intestinal environment (FaSSIF pH 6.5), were effective in screening cocrystal performance *in vitro* and predicting that cocrystals are more tolerant to elevated pH than the solid drug. Among the three KTZ cocrystals evaluated *in vitro*, the KTZ-SUC was selected for *in vivo* investigation in beagle dogs due to its high and sustained supersaturation *in vitro*. While KTZ exhibited high sensitivity to elevated gastric pH *in vivo*, its succinic acid cocrystal lowered this sensitivity by an order of magnitude. In fact, the cocrystal AUC and C_{max} values under elevated pH were similar to those of KTZ under acidic gastric pH, highlighting the potential of cocrystals to improve drug exposure under elevated gastric pH conditions.

CRediT authorship contribution statement

Yitian Marguerite Tucci: Writing – review & editing, Methodology, Investigation, Formal analysis, Conceptualization. **Tatiane Cogo Machado:** Writing – review & editing, Writing – original draft, Methodology, Formal analysis, Conceptualization. **Duxin Sun:** Writing – review & editing, Methodology, Formal analysis, Conceptualization. **Naír Rodríguez-Hornedo:** Writing – review & editing, Supervision, Project administration, Methodology, Formal analysis, Conceptualization.

Acknowledgements

Research reported in this publication was partially supported by the National Institute of General Medical Sciences on the National Institutes of Health under award number R01GM107146. The content is solely the responsibility of the authors and does not necessarily represent the official views of the National Institutes of Health. We also acknowledge the Gordon and Pamela Amidon Fellowship in Pharmaceutics, the Norman Weiner Graduate Scholarship, and the Warner-Lambert/Parke-Davis Fellowship, at the University of Michigan, College of Pharmacy. We gratefully acknowledge Dr. Gislaine Kuminek for her contributions in the preparation of doses for the *in vivo* beagle dog study and Dr. Bo Wen for overseeing the PK studies.

Supplementary materials

Supplementary material associated with this article can be found, in the online version, at doi:10.1016/j.ejps.2026.107550.

Data availability

Data will be made available on request.

References

Amidon, G.L., Tsume, Y., 2017. Oral product input to the GI tract: GIS an oral product performance technology. Front. Chem. Sci. Eng. https://doi.org/10.1007/s11705-017-1658-7.
Avdeef, A., 2012. pKa determination. Avdeef, Alex. Absorption and Drug Development: Solubility, Permeability and Charge State, 2nd ed. Wiley.
Bevernage, J., Brouwers, J., Annaert, P., Augustijns, P., 2012. Drug precipitation-permeation interplay: Supersaturation in an absorptive environment. Euro. J. Pharma. Biopharm. 82, 424–428. https://doi.org/10.1016/j.ejpb.2012.07.009.
Cao, F., Rodriguez-Hornedo, N., Amidon, G.E., 2019. Mechanistic Analysis of Cocrystal Dissolution, Surface pH, and Dissolution Advantage as a Guide for Rational Selection. J. Pharm. Sci. 108, 243–251. https://doi.org/10.1192/bjp.112.483.211-a.
Chen, Y., Rodríguez-Hornedo, N., 2018. Cocrystals Mitigate Negative Effects of High pH on Solubility and Dissolution of a Basic Drug. Cryst. Growth Des. 18, 1358–1366. https://doi.org/10.1021/acs.cgd.7b01206.
Chen, Y.M., 2017. Cocrystals Mitigate the Effect of pH on Solubility and Dissolution of Basic Drugs (PhD Thesis). University of Michigan.
Chin, T.W.F., Loeb, M., Fong, I.W., 1995. Effects of an Acidic Beverage (Coca-Cola) on Absorption of Ketoconazole. Antimicrob. Agents Chemother. 39, 1671–1675. https://doi.org/10.1128/AAC.39.8.1671.
Dressman, J., Berardi, R.R., Dermentzoglou, L.C., Russell, T.L., Schmaltz, S.P., Barnett, J. L., Jarvenpaa, K.M., 1990. Upper Gastrointestinal (GI) pH in Young, Healthy Men and Women. Pharm. Res. 7, 756–761.
Dressman, J.B., Reppas, C., 2000. In vitro-in vivo correlations for lipophilic, poorly water-soluble drugs. Euro. J. Pharma. Sci. https://doi.org/10.1016/S0928-0987(00)00181-0.
Fancher, R.M., Zhang, H., Sleczka, B., Derbin, G., Rockar, R., Marathe, P., 2011. Development of a canine model to enable the preclinical assessment of pH-dependent absorption of test compounds. J. Pharm. Sci. 100, 2979–2988. https://doi.org/10.1002/jps.22486.
Galia, E., Nicolaides, E., Hörter, D., Löbenberg, R., Reppas, C., Dressman, J.B., 1998. Evaluation of various dissolution media for predicting In vivo performance of class I and II drugs. Pharm. Res. https://doi.org/10.1023/A:1011910801212.
Good, D.J., Rodríguez-Hornedo, N., 2010. Cocrystal eutectic constants and prediction of solubility behavior. Cryst. Growth Des. 10, 1028–1032. https://doi.org/10.1021/cg901232h.
Good, D.J., Rodríguez-Hornedo, N., 2009. Solubility advantage of pharmaceutical cocrystals. Cryst. Growth Des. 9, 2253–2264. https://doi.org/10.1021/cg801039j.
Higashino, H., Minami, K., Takagi, T., Kataoka, M., Yamashita, S., 2023. The effects of degree and duration of supersaturation on in vivo absorption profiles for highly permeable drugs, dipyridamole and ketoconazole. Eur. J. Pharmaceut. Biopharmaceut. 189, 48–55. https://doi.org/10.1016/j.ejpb.2023.06.002.
Kostewicz, E.S., Wunderlich, M., Brauns, U., Becker, R., Bock, T., Dressman, J.B., 2004. Predicting the precipitation of poorly soluble weak bases upon entry in the small intestine. J. Pharm. Pharmacol. 56, 43–51. https://doi.org/10.1211/0022357022511.
Koziolek, M., Grimm, M., Bollmann, T., Schäfer, K.J., Blattner, S.M., Lotz, R., Boeck, G., Weitschies, W., 2019. Characterization of the GI transit conditions in Beagle dogs with a telemetric motility capsule. Euro. J. Pharma. Biopharm. 136, 221–230. https://doi.org/10.1016/j.ejpb.2019.01.026.
Kuminek, G., Rodríguez-Hornedo, N., Siedler, S., Rocha, H.V.A., Cuffini, S.L., Cardoso, S. G., 2016. How cocrystals of weakly basic drugs and acidic coformers might modulate solubility and stability. Chem. Comm. 52, 5832–5835. https://doi.org/10.1039/c6cc00898d.
Leyssens, T., Horst, J.H., 2018. Solution co-crystallisation and its applications. In: Tiekink, E., Zukerman-Schpector, J. (Eds.), Multi-Component Crystals. Walter de Gruyter GmbH, Berlin/Boston Coverf, Berlin/Boston, pp. 205–236. https://doi.org/10.1002/9781119109785.pubnote.

Martin, F.A., Pop, M.M., Borodi, G., Filip, X., Kacso, I., 2013. Ketoconazole salt and co-crystals with enhanced aqueous solubility. Cryst. Growth Des. 13, 4295–4304. https://doi.org/10.1021/cg400638g.

Mathias, N.R., Xu, Y., Patel, D., Grass, M., Caldwell, B., Jager, C., Mullin, J., Hansen, L., Crison, J., Saari, A., Gesenberg, C., Morrison, J., Vig, B., Raghavan, K., 2013. Assessing the risk of pH-dependent absorption for new molecular entities: A novel in vitro dissolution test, physicochemical analysis, and risk assessment strategy. Mol. Pharm. 10, 4063–4073. https://doi.org/10.1021/mp400426f.

Mitra, A., Kesisoglou, F., Beauchamp, M., Zhu, W., Chiti, F., Wu, Y., 2011. Using absorption simulation and gastric pH modulated dog model for formulation development to overcome achlorhydria effect. Mol. Pharm. 8, 2216–2223. https://doi.org/10.1021/mp200062a.

Mudie, D.M., Amidon, G.L., Amidon, G.E., 2010. Physiological parameters for oral delivery and in vitro testing. Mol. Pharm. https://doi.org/10.1021/mp100149j.

Park, M.J., Ren, S., Lee, B.J., 2007. In vitro and in vivo comparative study of intraconazole bioavailability when formulated in highly soluble self-emulsifying system and in solid dispersion. Biopharm. Drug Dispos. 28, 199–207. https://doi.org/10.1002/bdd.546.

Patel, S., Zhu, W., Xia, B., Sharma, N., Hermans, A., Ehrick, J.D., Kesisoglou, F., Pennington, J., 2019. Integration of Precipitation Kinetics From an In Vitro, Multicompartment Transfer System and Mechanistic Oral Absorption Modeling for Pharmacokinetic Prediction of Weakly Basic Drugs. J. Pharm. Sci. 108, 574–583. https://doi.org/10.1016/j.xphs.2018.10.051.

Piscitelli, S.C., Goss, T.F., Wilton, J.H., D'andrea, D.T., Goldstein, H., Schentag', J.J., 1991. Effects of Ranitidine and Sucralfate on Ketoconazole Bioavailability. Antimicrob. Agents Chemother. 35, 1765–1771. https://doi.org/10.1128/AAC.35.9.1765.

Plum, J., Bavnhøj, C., Palmelund, H., Pérez-Alós, L., Müllertz, A., Rades, T., 2020. Comparison of induction methods for supersaturation: pH shift versus solvent shift. Int. J. Pharm. 573, 118862. https://doi.org/10.1016/j.ijpharm.2019.118862.

Rodríguez-Hornedo, N., Nehm, S.J., Seefeldt, K.F., Pagán-Torres, Y., Falkiewicz, C.J., 2006. Reaction crystallization of pharmaceutical molecular complexes. Mol. Pharm. 3, 362–367. https://doi.org/10.1021/mp050099m.

Ruff, A., Fiolka, T., Kostewicz, E.S., 2017. Prediction of Ketoconazole absorption using an updated in vitro transfer model coupled to physiologically based pharmacokinetic modelling. Euro. J. Pharma. Sci. 100, 42–55. https://doi.org/10.1016/j.ejps.2016.12.017.

Russell, T.L., Berardi, R.R., Barnett, J.L., O'Sullivan, T.L., Wagner, J.G., Dressman, J.B., 1993. pH-Related Changes in the Absorption of Dipyridamole in the Eldery. Pharm Res 11, 136–143. https://doi.org/10.1023/a:1018918316253.

Santos Goes, A.K., Soliman, A., Kowthavarapu, V.K., Oliveira, P.R., de Moraes, N.V., 2026. Enhancing bioavailability of a weakly basic drug through cocrystallization: PBPK modeling of ketoconazole–succinic acid. Euro. J. Pharma. Biopharm. 220, 114986. https://doi.org/10.1016/j.ejpb.2026.114986.

Streubel, A., Siepmann, J., Dashevsky, A., Bodmeier, R., 2000. pH-independent release of a weakly basic drug from water-insoluble and-soluble matrix tablets. J. Control. Release. 67, 101–110. https://doi.org/10.1016/s0168-3659(00)00200-5.

Takano, R., Sugano, K., Higashida, A., Hayashi, Y., Machida, M., Aso, Y., Yamashita, S., 2006. Oral absorption of poorly water-soluble drugs: Computer simulation of fraction absorbed in humans from a miniscale dissolution test. Pharm. Res. 23, 1144–1156. https://doi.org/10.1007/s11095-006-0162-4.

Tsume, Y., Matsui, K., Searls, A.L., Takeuchi, S., Amidon, G.E., Sun, D., Amidon, G.L., 2017. The impact of supersaturation level for oral absorption of BCS class IIb drugs, dipyridamole and ketoconazole, using in vivo predictive dissolution system: Gastrointestinal Simulator (GIS). Euro. J. Pharma. Sci. 102, 126–139. https://doi.org/10.1016/j.ejps.2017.02.042.

Van der Meer, J.W., Keuning, J.J., Scheijgrond, H.W., Heykants, J., Van Cutsem, J., Brugmans, J., 1980. Influence of gastric acidity on the bioavailability of ketoconazole. J. Antimicro. 6, 552–554. https://doi.org/10.1093/jac/6.4.552.

Zhou, R., Moench, P., Heran, C., Lu, X., Mathias, N., Faria, T.N., Wall, D.A., Hussain, M. A., Smith, R.L., Sun, D., 2005. pH-Dependent dissolution in Vitro and absorption in Vivo of weakly basic drugs: Development of a canine model. Pharm. Res. 22, 188–192. https://doi.org/10.1007/s11095-004-1185-3.